A DNA nanosensor for monitoring ligand-induced i-motif formation

Article *in* Organic & Biomolecular Chemistry · February 2021

DOI: 10.1039/D1OB00248A

4 authors:

Puja Saha
Indian Association for the Cultivation of Science
17 PUBLICATIONS **191** CITATIONS
SEE PROFILE

Deepanjan Panda
Indian Association for the Cultivation of Science
15 PUBLICATIONS **275** CITATIONS
SEE PROFILE

Raj Paul
Indian Association for the Cultivation of Science
8 PUBLICATIONS **40** CITATIONS
SEE PROFILE

Jyotirmayee Dash
Indian Association for the Cultivation of Science
142 PUBLICATIONS **3,156** CITATIONS
SEE PROFILE

Organic & Biomolecular Chemistry

ROYAL SOCIETY OF CHEMISTRY

COMMUNICATION

View Article Online
View Journal | View Issue

Cite this: *Org. Biomol. Chem.*, 2021, **19**, 1965

Received 6th January 2021,
Accepted 9th February 2021

DOI: 10.1039/d1ob00248a

rsc.li/obc

A DNA nanosensor for monitoring ligand-induced i-motif formation†

Puja Saha, Deepanjan Panda, Raj Paul and Jyotirmayee Dash *

Herein, we present a gold nanoparticle (GNP)-based DNA nanosensor to detect the formation of an i-motif from the random coil structure by small molecules at physiological pH. The nanosensor shows a distance dependent fluorescence turn-off response in the presence of a ligand, indicating conformational changes from the C-rich single stranded DNA into an i-motif.

i-Motifs are interspersed tetrahelical DNA secondary structures that are stabilized by hemi-protonated and intercalated cytosine base pairs ($C:C^+$).[1–4] The *in vitro* stability of i-motifs strongly depends on chemical and physical environmental factors such as acidic pH, low ionic strength, molecular crowding, low temperature, *etc.*[1–4] These conditions are not available in cellular environment to stabilize i-motif structures. Thus, the existence of i-motifs within genomic DNA is still a matter of scientific debate. Recent studies show that i-motifs are stable and they exist in the nuclei of living human cells.[5–7] These findings suggest that i-motifs could be potential targets for gene regulations. The non-canonical DNA i-motifs are also hypothesized to be involved in several cancer-related processes.[8,9] In this regard, ligands that preferentially target and induce the i-motif formation in genomic DNA in the cellular environment would be useful in i-motif-targeted anti-cancer therapeutics. Such ligands[10–16] would also provide detailed insights into the potential impact of i-motif structures on physiological processes. Thus a simple and fast high-throughput screening method can be used to identify i-motif inducing ligands at physiological pH.

Circular Dichroism, ^{1}H NMR spectroscopy and FRET-based techniques (like FRET-based DNA melting assay, smFRET, *etc.*)[10–16] are currently used as standard methods to detect ligand mediated i-motif formation and stabilization. However, NMR and CD spectroscopy techniques are time-consuming, have low throughput and require precise control of experimental setups. FRET based assays are generally used to detect i-motif stabilization under acidic conditions. In comparison to these traditional detection methods, gold nanoparticle (GNP)-based nanosensors are extremely attractive because of the ease of detection, minimal interference, high sensitivity and potential for high-throughput analysis.

GNP-based sensors are of particular interest due to the unique features of gold nanomaterials such as distinct optical and physicochemical properties, controllable size, ease of synthesis and versatile surface chemistry that allow multifunctionalization with a wide range of organic or biological molecules.[17–23] Each of these attributes of GNPs enables researchers to develop novel cost effective probes for the selective binding and detection of small molecules and biological targets.[17–27] We herein report the design and fabrication of a high throughput GNP-based DNA sensor for the identification of i-motif inducing ligands. To our knowledge, GNP-based sensors have not been reported so far to detect induction of the i-motif structure at physiological pH.

In this study, the GNP-based DNA probe was devised by grafting random coil cytosine-rich DNA sequences onto the surface of water-soluble gold nanoparticles (GNPs) *via* thiol–gold covalent bonds (Fig. 1). We have used a 5′-thiolated C-rich

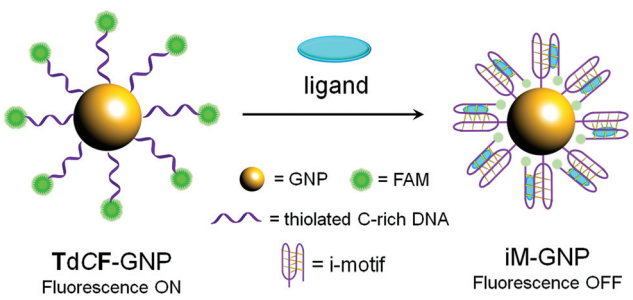

TdCF: 5′-ThiC6-$TC_4AC_2T_2C_4AC_3TC_4AC_3TC_4A$-FAM-3′

Fig. 1 Schematic illustration for the detection of ligand-mediated i-motif folding using gold nanoparticles (GNPs) coated with 5′-thiolated and 3′-FAM labelled C-rich DNA sequences.

School of Chemical Sciences, Indian Association for the Cultivation of Science, Jadavpur, Kolkata-700032, India. E-mail: ocjd@iacs.res.in; Fax: +91-33-2473-2805; Tel: +91-33-2473-4971, ext 1405

†Electronic supplementary information (ESI) available. See DOI: 10.1039/d1ob00248a

Table 1 DNA sequences used

DNA	Sequence (5′.....3′)
C-rich DNA	$TC_4AC_2T_2C_4AC_3TC_4AC_3TC_4A$ [10 mM sodium cacodylate, 10 mM NaCl, pH 5.5; i-motif (iM)] [MilliQ water; single stranded C rich DNA (ss*C*)]
T*d**C**F*	**ThiC6**-$TC_4AC_2T_2C_4AC_3TC_4AC_3TC_4A$-**FAM** [MilliQ water]
F*d**C**T′*	**FAM**-$TC_4AC_2T_2C_4AC_3TC_4AC_3TC_4A$-**TAMRA**
T*d**C**F*·d*G*	Strand 1: **ThiC6**-$TC_4AC_2T_2C_4AC_3TC_4AC_3TC_4A$-**FAM**; T*d**C**F* Strand 2: $TG_4AG_3TG_4AG_3TG_4A_2G_2TG_4A$; d*G* [10 mM Tris. HCl, pH 8]
d*C*·d*G*	Strand 1: $TC_4AC_2T_2C_4AC_3TC_4AC_3TC_4A$; d*C* Strand 2: $TG_4AG_3TG_4AG_3TG_4A_2G_2TG_4A$; d*G* [10 mM Tris. HCl, pH 8]

DNA (T*d**C**F*), which is tagged with FAM at 3′-end (Table 1). GNPs were synthesized through the reduction of $HAuCl_4$ *via* sodium citrate.[28] The GNPs are around 40 nm in size (Fig. S1†) and contain ~120 strands per particle. The DNA-grafted GNP nanosensor generates a distance-dependent fluorescence quenching signal in response to the i-motif formation by a ligand. When T*d**C**F* DNA (Table 1) is in the unfolded state, the tagged fluorophore remains away from the GNP surface giving a high fluorescence response. The folding of T*d**C**F* into an i-motif (iM) in the presence of a ligand brings the fluorophore close to the GNP surface that quenches the FAM fluorescence (Fig. 1). This indicates the ligand's ability to induce the formation of an i-motif from the random coil C-rich DNA.

We have used a pyrrolidine mono-triazolyl carbazole derivative, ligand **1**, which was developed by *in situ* cycloaddition using an i-motif DNA-nanotemplate.[29] Fluorescence studies revealed that **1** shows high affinity for i-motifs with a K_d value of 0.25 μM (Fig. S2†). Interestingly, Förster Resonance Energy Transfer (FRET) melting analysis[30] revealed that ligand **1** is capable of folding a C-rich sequence to an i-motif under physiological conditions. In the FRET study, a dual-labeled C-rich DNA sequence (F*d**C**T′*) was used under both folded (pH 5.5, iM) and unfolded (pH 7.4, ss*C*) conditions. At acidic pH (pH 5.5), the i-motif (iM) exhibited a T_m value of 47.5 °C, while the C-rich DNA (ss*C*) remained unfolded at pH 7.4, showing no measurable T_m value (<37 °C) (Fig. S3a and b†). At pH 5.5, **1** significantly stabilized the i-motif, showing a ΔT_m value of 18 °C (T_m of 65.5 °C) at 0.5 μM concentration and a ΔT_m of 29.5 °C (T_m of 77 °C) at 1 μM concentration (Fig. S3a†). Moreover, it showed a maximum stabilization potential for iM (T_m of 93 °C) at a concentration of 3 μM (Fig. S3a†). FRET studies further illustrated that **1** gradually increased the T_m values of unfolded C-rich DNA (ss*C*) at physiological pH. It was observed that the T_m of F*d**C**T′* (pH 7.4, ss*C*) increased to 58.5 °C at 1 μM, 78.4 °C at 5 μM and 82.3 °C at 10 μM concentration of **1** (Fig. S3b†). These results indicated that **1** is able to stabilize the i-motif structure and is also able to fold the unfolded form (ss*C*) into an i-motif (iM) at physiological pH.

Circular Dichroism (CD) spectroscopy further confirmed the ability of **1** to fold the i-motif structure. The C-rich DNA (d*C*) folded at pH 5.5 (*i.e.* the iM DNA) showed a positive maximum at 288 nm and a negative peak in the range of 260–267 nm in the CD spectrum, corresponding to a typical i-motif conformation[31] (Fig. S3c†). Upon addition of **1**, no spectral shift was observed, suggesting that **1** stabilizes iM and does not perturb its conformation. At pH 7.4, the CD spectrum of C-rich oligonucleotides (ss*C*) showed a positive signal at 277 nm and a negative signal at 236 nm, indicative of a random coil type structure (Fig. S3d†). Upon addition of **1**, gradual bathochromic shifts in both positive and negative signals were observed. With increasing concentrations of **1** (0 to 1 equiv.), the negative peak at 236 nm was shifted to 261 nm, and the positive maximum was red-shifted to 288 nm with an increase in ellipticity (Fig. S3d†). This reveals that **1** could promote and stabilize the folded conformation of i-motif DNA under neutral and acidic conditions.

Next, the efficacy of the DNA nanosensor to detect the iM formation from the random coil structure (ss*C*) by ligand **1** was monitored by fluorescence spectroscopy (Fig. 2a). The DNA-linked GNPs (T*d**C**F*-GNP) exhibit a strong characteristic fluorescence signal for FAM (λ_{ex} = 488 nm and λ_{em} = 542 nm) at physiological pH (Fig. 2b). Upon addition of **1**, a noticeable decrease in fluorescence intensity of FAM was observed (Fig. 2b and c) and the fluorescence signal was quenched by 5-fold in the presence of 1 μM of **1** (Fig. 2d). The quenching may arise from the molecular interactions between FAM and ligand **1**. However, fluorescence titrations of free T*d**C**F* DNA (not grafted on GNPs) with the ligand **1** showed only a 1.4-fold decrease in the fluorescence intensity of FAM (Fig. S4†). Taken together, these results indicate that the observed fluorescence quenching of the GNP-based system is due to the folding of the random C-rich coil into the i-motif conformation by **1**.

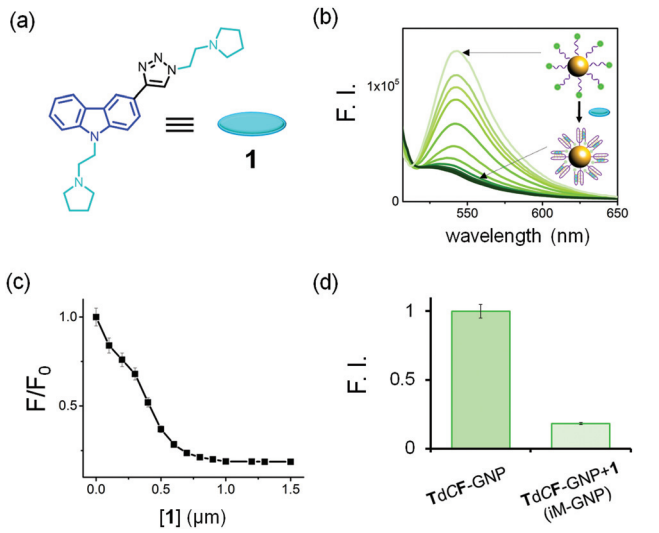

Fig. 2 (a) Chemical structure of **1**. (b) Fluorescence titration of T*d**C**F* DNA linked GNPs (T*d**C**F*-GNP) with **1** showing fluorescence quenching and induction of i-motif formation on the GNP surface (DNA conc. 100 nM). λ_{ex} = 488 nm, milliQ water (c) normalized fluorescence response of T*d**C**F*-GNP in the presence of increasing concentrations of **1**. (d) Bar diagram showing the normalized fluorescence responses of T*d**C**F*-GNP alone and **1** bound T*d**C**F*-GNP (iM-GNP).

To further examine the sensitivity of the GNP-based system, we developed a *ligand-specific* label-free fluorescence based assay by employing Thioflavin T (ThT) as a signal transducer. ThT, containing benzothiazole and dimethylaminobenzene rings, has been reported as a fluorescent sensor for human i-motif DNA.[32] ThT showed negligible fluorescence changes with ss*C* at pH 7.4 and exhibited a 6-fold fluorescence enhancement with the iM DNA (pre-folded at pH 5.5) (Fig. S5†). These observations indicate that ThT selectively interacts with the i-motif structure (iM) over a single stranded C-rich oligonucleotide (ss*C*). In contrast, ligand **1** is initially fluorescent and its fluorescence was quenched significantly upon addition of either the random coil C-rich DNA (ss*C*, pH 7.4) (Fig. S6†) or the iM DNA (pre-folded at pH 5.5) (Fig. S2†).[25] We further observed that **1** and ThT could be a possible donor–acceptor pair as the absorption spectrum of ThT (λ_{ex} = 412 nm and λ_{em} = 486 nm) overlaps with the emission spectrum of **1** (λ_{ex} = 290 nm and λ_{em} = 375 nm).

Molecular docking studies revealed that **1** interacted with the groove region of an i-motif (PDB: 1YBL[33]) with a binding energy of −10.16 kcal mol^{-1} (Fig. S7†). ThT could bind to another groove region of the i-motif with a binding energy of −4.77 kcal mol^{-1}. Docking studies performed with both the ligands illustrated that **1** and ThT could simultaneously bind at different groove regions of an i-motif structure (Fig. S7†). We, therefore, hypothesized that if **1** could induce the i-motif formation at physiological pH, ThT would then exhibit a fluorescence turn-on response upon interaction with i-motif DNA (folded by **1**) at pH 7.4 (Fig. 3a). In this context, we prepared a mixture of **1** (100 nM) and ThT (1 μM) and monitored the fluorescence spectra of the resulting mixture upon excitation at 290 nm (λ_{ex} of **1**) (Fig. 3b). Upon incremental addition of ss*C* to this mixture at pH 7.4, the fluorescence intensity of **1** (λ_{em} = 375 nm) gradually quenched, and simultaneously, there was an increase in the fluorescence intensity of ThT (λ_{em} = 486 nm). This suggests that iM was formed from ss*C* by **1** and then ThT interacted with iM DNA, exhibiting a turn-on response (Fig. 3b and c). In addition, the fluorescence intensity of ThT was not altered with the gradual addition of **1**, indicating no molecular interactions between ThT and **1**. Collectively, these studies illustrate that **1** can induce and stabilize i-motif DNA at physiological pH and further indicate that the GNP-based method can be used for screening of compounds to identify ligands with the ability to induce the i-motif formation.

We then focussed our attention on devising a DNA nanosensor to investigate the i-motif formation from G·C-rich duplex DNA. Double stranded regions of the human genome can adopt iM/G$_4$ structures, and the formation of these structures is in equilibrium with duplex DNA.[34] In order to prepare the nanosensor, we first immobilized G·C-rich duplex DNA (**Td*C*F**·d*G*) on the surface of GNPs (Fig. 4a). The duplex DNA (**Td*C*F**·d*G*) was prepared by annealing the 5′-thiol and 3′-FAM containing **Td*C*F** sequence and its complementary untagged d*G* DNA sequence in 10 mM Tris·HCl buffer, pH 8. The **Td*C*F**·d*G* DNA-grafted GNP system (**Td*C*F**·d*G*-GNP) showed a high FAM fluorescence (Fig. 4b). Upon gradual addition of **1**,

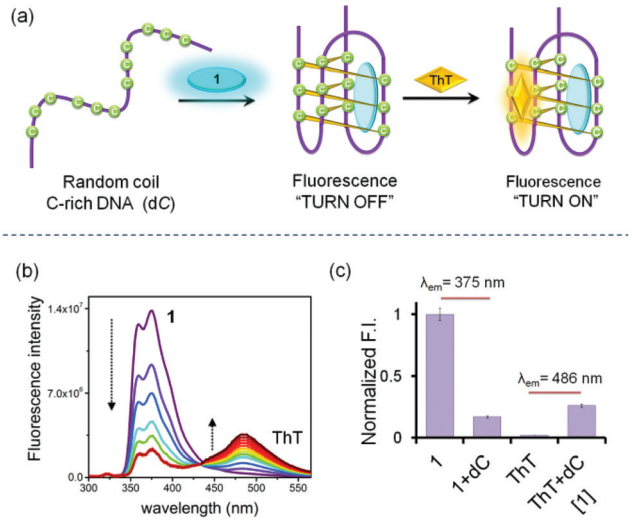

Fig. 3 (a) Proposed mechanism for the induction and stabilization of the i-motif structure by **1** and subsequent binding to Thioflavin T (ThT) showing a fluorescence turn-on response. (b) Fluorimetric curves of **1** (0.1 μM) and ThT (1 μM) [excitation at 290 nm] with the ss*C* sequence (milliQ water). (c) Diagram of the normalized fluorescence intensities of **1** and ThT alone and with DNA at 375 nm and 486 nm, respectively.

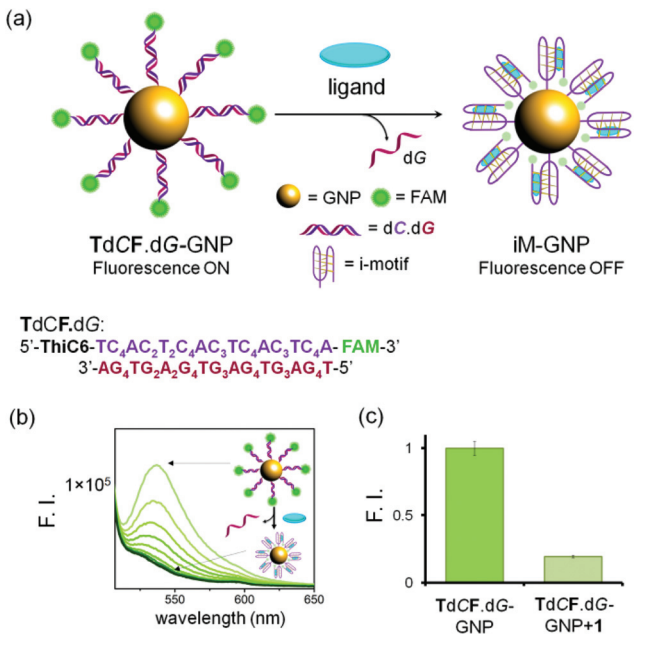

Fig. 4 (a) Schematic representation of the designed FAM-tagged G·C-rich duplex DNA immobilized GNPs (**Td*C*F**·d*G*-GNP) to detect the formation of the i-motif. (b) Fluorescence titration of G·C-rich duplex DNA linked GNPs (**Td*C*F**·d*G*-GNP) with **1** showing fluorescence quenching and induction of the i-motif formation on the GNP surface [DNA conc. 200 nM (100 nM **Td*C*F** and 100 nM d*G*)]. λ_{ex} = 488 nm, buffer: 10 mM Tris·HCl buffer, pH 8. (c) Bar diagram showing the normalized fluorescence responses of **Td*C*F**·d*G*-GNP alone and with **1**.

the fluorescence signal of the DNA sensor was significantly quenched 5.2-fold (Fig. 4c). However, the fluorescence response of FAM was not considerably altered when **1** was titrated with **T**d*C***F**·d*G* DNA, Fig. S8.† These further indicate that **1** is able to promote i-motif folding from G·C-rich duplex DNA.

The underlying reason for the quenching was studied using a well-known anticancer agent doxorubicin (Dox). Dox showed fluorescence quenching in the presence of duplex DNA, G-quadruplex and i-motif DNA as well as with unfolded G-rich and C-rich DNA (Fig. S9–S12†).[35] Free Dox exhibited an intrinsic high fluorescence signal (λ_{ex} = 480 nm and λ_{em} = 590 nm) and upon incremental addition of d*C*·d*G* duplex DNA (sequence listed in Table 1), a dramatic decrease in the fluorescence intensity of Dox was observed (Fig. 5a). Intriguingly, upon addition of **1** in this state (Fig. 5b), it was observed that the fluorescence intensity of the Dox-d*C*·d*G* DNA complex was increased. These results suggested that **1** could release Dox from duplex DNA and restore the fluorescence of Dox. We also observed that the fluorescence intensity of free Dox was hardly altered in the presence of **1**, indicating negligible molecular interactions between Dox and **1** (Fig. S13†). CD experiments were further performed with d*C*·d*G* DNA and ligand **1** to validate the formation of the i-motif from duplex DNA. The d*C*·d*G* duplex DNA exhibited a positive peak at 270 nm and a negative peak at 240 nm. In the presence of 5 eq. of ligand **1**, a broad positive band with a significant decrease in molar ellipticity was observed. We have hypothesized that this kind of broad spectrum may arise from a mixture of unfolded and/or partially folded structures (Fig. S14†). Upon addition of a higher concentration of **1** (10 eq.), a spectrum of mixed peaks appeared: a major peak at 288 nm, which corresponds to the i-motif conformation and a broad minor peak near 250–265 nm, which may correspond to unstructured single-stranded topology and/or G-quadruplex structures. Based on these results, we could infer that the duplex DNA conformation is perturbed in the presence of **1**, thereby triggering the formation of stable i-motif DNA (Fig. 5c).

To investigate the applicability of the **T**d*C***F**-GNP system, we next carried out a screening experiment with a library of 25 structurally relative carbazole derivatives (**1–25**) (Fig. S15†) for their ability to induce the i-motif formation. In the screening, un-annealed C-rich DNA grafted GNPs (**T**d*C***F**-GNP) were mixed with 1.0 μM of each ligand in 10 mM sodium cacodylate buffer, 10 mM NaCl, pH 7.4 in multi-well plates. After 30 min incubation, in the dark, the fluorescence intensities of each well were recorded. For each ligand, control experiments were carried out by monitoring the fluorescence response of the mixture of ligand and free C-rich random coil in the same buffer, indicating whether the ligands would have some intrinsic quenching effect on FAM fluorescence. By monitoring the normalized fluorescence quenching for each ligand (Fig. S16†), we observed that ligand **1** was the top hit in this screening, showing 69% fluorescence quenching. The next-best hit after **1** was found to be **8** containing aliphatic amine chains, showing a quenching of 56% followed by **5** that exhibits a fluorescence quenching by only 20%. To validate the results, FRET melting assay was performed with these ligands (1 μM conc.) at pH 7.4. Of all the ligands tested, **1** has the highest T_m value (58.5 °C) for **F**d*C***T**′ DNA (T_m < 37 °C; could not be determined), followed by **8** (T_m = 43.7 °C) and **5** (T_m = 38.3 °C). Other carbazole ligands did not show any difference in the melting temperature of C-rich random coil DNA. The FRET melting results are consistent with the GNP-based screening, indicating the applicability of the sensor to identify i-motif inducing ligands at physiological pH.

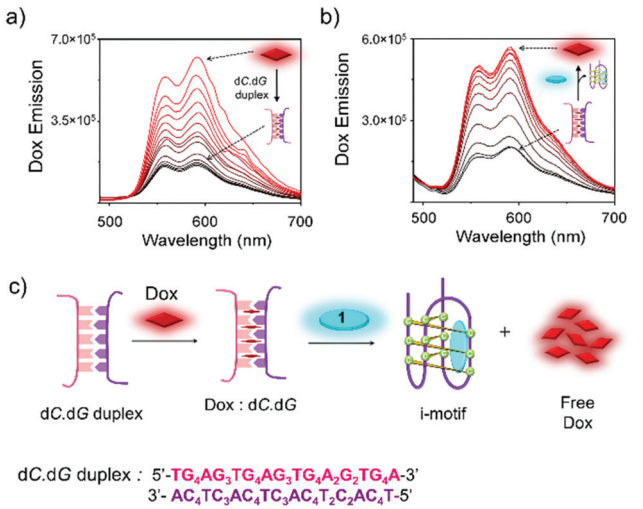

Fig. 5 (a) Fluorescence titration of Dox with d*C*·d*G* duplex DNA showing a decrease in fluorescence intensity (λ_{ex} = 480 nm, buffer 10 mM Tris·HCl, pH 8). (b) Restoration of Dox fluorescence after addition of **1**, which converts the d*C*·d*G* duplex into i-motif DNA. (a) Schematic representation of **1** induced i-motif formation from G·C rich duplex DNA (d*C*·d*G*) and subsequent release of Dox.

Conclusions

In summary, we have developed a GNP-based DNA nanosensor for the identification of ligands capable of triggering the i-motif formation from a random coil C-rich DNA sequence at physiological pH. The DNA nanosensor produces conformation-specific fluorescence readout in the presence of an i-motif inducing ligand. However, a ligand may interact with the fluorophore of the nanoprobe, which can cause undefined changes in fluorescence. This can be nullified by monitoring the fluorescence response of free FAM tagged DNA in the presence of a ligand. It is noteworthy to state that the ligand should not have any spectral overlap with the used fluorophore, so careful selection of the fluorophore is highly desirable. The UV–vis absorbance of the tested ligands should be examined to invalidate these misleading observations. Nevertheless, this assay could be considered as a reliable and high-throughput screening method for the identification of i-motif folding and stabilizing ligands. Moreover, we also envisage that this GNP-based screening platform could find versatile applications in designing biomolecular nano-devices.

Conflicts of interest

There are no conflicts to declare.

Acknowledgements

JD thanks Wellcome Trust-DBT India Alliance (Grant Number, IA/S/18/2/503986) for funding. RP thanks DST for the INSPIRE fellowship. The authors thank Dr. Sandipan Chakraborty for performing the molecular docking studies.

References

1 K. Gehring, J. L. Leroy and M. Gueron, *Nature*, 1993, **363**, 561.
2 J. L. Leroy, M. Gueron, J. L. Mergny and C. Helene, *Nucleic Acids Res.*, 1994, **22**, 1600.
3 S. Benabou, A. Avino, R. Eritja, C. Gonzalez and R. Gargallo, *RSC Adv.*, 2014, **4**, 26956–26980.
4 H. Abou Assi, M. Garavis, C. Gonzalez and M. J. Damha, *Nucleic Acids Res.*, 2018, **46**, 8038.
5 E. P. Wright, J. L. Huppert and Z. A. E. Waller, *Nucleic Acids Res.*, 2017, **45**, 2951.
6 S. Dzatko, M. Krafcikova, R. Hansel-Hertsch, T. Fessl, R. Fiala, T. Loja, D. Krafcik, J. L. Mergny, S. Foldynova-Trantirkova and L. Trantirek, *Angew. Chem., Int. Ed.*, 2018, **57**, 2165.
7 M. Zeraati, D. B. Langley, P. Schofield, A. L. Moye, R. Rouet, W. E. Hughes, T. M. Bryan, M. E. Dinger and D. Christ, *Nat. Chem.*, 2018, **10**, 631.
8 M. Debnath, K. Fatma and J. Dash, *Angew. Chem., Int. Ed.*, 2019, **58**, 2942.
9 J. Amato, N. Iaccarino, A. Randazzo, E. Novellino and B. Pagano, *ChemMedChem*, 2014, **9**, 2026.
10 X. Li, Y. H. Peng, J. S. Ren and X. G. Qu, *Proc. Natl. Acad. Sci. U. S. A.*, 2006, **103**, 19658.
11 X. Chen, X. J. Zhou, T. Han, J. Y. Wu, J. Y. Zhang and S. W. Guo, *ACS Nano*, 2013, **7**, 531.
12 E. P. Wright, H. A. Day, A. M. Ibrahim, J. Kumar, L. J. E. Boswell, C. Huguin, C. E. M. Stevenson, K. Pors and Z. A. E. Waller, *Sci. Rep.*, 2016, **6**, 39456.
13 M. Debnath, S. Ghosh, A. Chauhan, R. Paul, K. Bhattacharyya and J. Dash, *Chem. Sci.*, 2017, **8**, 7448.
14 S. Kendrick, H. J. Kang, M. P. Alam, M. M. Madathil, P. Agrawal, V. Gokhale, D. Z. Yang, S. M. Hecht and L. H. Hurley, *J. Am. Chem. Soc.*, 2014, **136**, 4161.
15 S. Satpathi, K. Das and P. Hazra, *Chem. Commun.*, 2018, **54**, 7054.
16 R. V. Brown, T. Wang, V. R. Chappeta, G. H. Wu, B. Onel, R. Chawla, H. Quijada, S. M. Camp, E. T. Chiang, Q. R. Lassiter, C. Lee, S. Phanse, M. A. Tumidge, P. Zhao, J. G. N. Garcia, V. Gokhale, D. Z. Yang and L. H. Hurley, *J. Am. Chem. Soc.*, 2017, **139**, 7456–7475.
17 K. Saha, S. S. Agasti, C. Kim, X. Li and V. M. Rotello, *Chem. Rev.*, 2012, **112**, 2739.
18 G. Zhang, *Nanotechnol. Rev.*, 2013, **2**, 269.
19 N. S. Abadeer and C. J. Murphy, *J. Phys. Chem. C*, 2016, **120**, 4691–4716.
20 A. J. Mieszawska, W. J. M. Mulder, Z. A. Fayad and D. P. Cormode, *Mol. Pharm.*, 2013, **10**, 831–847.
21 A. Heuer-Jungemann, P. K. Harimech, T. Brown and A. G. Kanaras, *Nanoscale*, 2013, **5**, 9503.
22 E. C. Dreaden, A. M. Alkilany, X. Huang, C. J. Murphy and M. A. El-Sayed, *Chem. Soc. Rev.*, 2012, **41**, 2740.
23 U. H. F. Bunz and V. M. Rotello, *Angew. Chem., Int. Ed.*, 2010, **49**, 3268.
24 M. S. Kang, S. Y. Lee, K. S. Kim and D.-W. Han, *Pharmaceutics*, 2020, **12**, 701.
25 A. F. Versiani, L. M. Andrade, E. M. Martins, S. Scalzo, J. M. Geraldo, C. R. Chaves, D. C. Ferreira, M. Ladeira, S. Guatimosim, L. O. Ladeira and F. G. da Fonseca, *Future Virol.*, 2016, **11**, 293.
26 L. Xian, H. Ge, N. Xu, F. Xu, Q. Yao, J. Fan, S. Long and X. Peng, *Ind. Eng. Chem. Res.*, 2020, **59**, 20582.
27 Y. Yang, J. Huang, X. Yang, X. He, K. Quan, N. Xie, M. Ou and K. Wang, *Anal. Chem.*, 2017, **89**, 5850.
28 K. C. Grabar, R. G. Freeman, M. B. Hommer and M. J. Natan, *Anal. Chem.*, 1995, **67**, 735.
29 P. Saha, D. Panda, D. Müller, A. Maity, H. Schwalbe and J. Dash, *Chem. Sci.*, 2020, **11**, 2058.
30 J. L. Mergny, *Biochemistry*, 1999, **38**, 1573.
31 G. Manzini, N. Yathindra and L. E. Xodo, *Nucleic Acids Res.*, 1994, **22**, 4634.
32 I. J. Lee, S. P. Patil, K. Fhayli, S. Alsaiari and N. M. Khashab, *Chem. Commun.*, 2015, **51**, 3747.
33 N. Esmaili and J.-L. Leroy, *Nucleic Acids Res.*, 2005, **33**, 213.
34 J. Zhou, S. Amrane, D. N. Korkut, A. Bourdoncle, H. Z. He, D. L. Ma and J. L. Mergny, *Angew. Chem., Int. Ed.*, 2013, **52**, 7742.
35 L. Scaglioni, R. Mondelli, R. Artali, F. R. Sirtori and S. Mazzini, *Biochim. Biophys. Acta*, 2016, **1860**, 1129.